Energy levels, transition rates, and line strengths of B-like ions

Liang-huan Hao and Gang Jiang*

Institute of Atomic and Molecular Physics, Sichuan University, Chengdu, 610065 Sichuan, People's Republic of China

(Received 19 October 2010; published 21 January 2011)

Extensive configuration interaction calculations for the $2s^22p-2s2p^2$ transitions for several ions along the B I isoelectronic sequence (Al IX, Mn XXI, Fe XXII, Co XXIII, Ni XXIV, Cu XXV, Zn XXVI, Mo XXXVIII, and Au LXXV) have been calculated using the GRASP2 K package based on the multiconfiguration Dirac-Hartree-Fock (MCDHF) method. By employing active-space techniques to expand the configuration list, we also included Breit interaction and quantum electrodynamical (QED) effects to correct atomic state wave functions and the corresponding energies. Both valence correlation and core polarization effects are included, the latter being significant in achieving agreement between length and velocity forms of the oscillator strengths of related allowed transitions. The fine-structure energy levels, term splitting, transition energies, transition rates, line strengths, and thereby the branching ratios are compared with experimental data and with values from other calculations.

DOI: 10.1103/PhysRevA.83.012511 PACS number(s): 31.30.Gs, 32.30.−r

I. INTRODUCTION

B-like ions are simple atomic systems for which interactions among the three outer electrons and interactions with an atomic core are important. Transitions from the configurations $2s^22p$ and $2s2p^2$ have been identified, and accurate transition energies are available. We note, in particular, the systematization efforts by Cheng [1], who by isoelectronic intercomparison provided recommended data with errors even smaller than those of the individual measurements. It is therefore of importance to develop reliable computational methods that can be used to supply these quantities. To provide for the extensive data needs, more large-scale calculations based on the many-body perturbation theory (MBPT) [2–4], the multiconfiguration Hartree-Fock (MCHF) [5–10], and the multiconfiguration Dirac-Hartree-Fock (MCDHF) [1,11–13] methods, together with today's powerful computers, have made it possible to calculate energy structures and transition probabilities in low-Z and intermediate-Z charged ions to very high accuracy [14–17]. A correspondingly large number of experimental studies of the energies of $n = 2$ states have been made using beam-foil techniques; for example, for Ti XVIII, Cr XX, Fe XXII, and Ni XXIV ions were identified in spectra obtained from Princeton Large Torus tokomak plasmas by Dave *et al.* [18]. More recently, this sequence was extended to Mo XXXVIII by Myrnäs *et al.* [19]. Highly charged uranium and thorium ions were produced in a high-energy electron-beam ion trap (SuperEBIT) at Lawrence Livermore National Laboratory [20,21], and their proper identification is important for plasma diagnostics in astrophysics as well as in fusion energy research.

When treating the $n = 2$ complex atoms and ions, one needs to account for the electron correlation effects, which play an extremely important role in the accurate description of low-Z and intermediate-Z ions. There, a significant Z-independent electron correlation contribution to the energy of a term exists. To include these correlation corrections as much as possible in the calculation of B-like isoelectronic sequence, Cheng *et al.* [1] carried out the calculation in the $n = 2$ complex in order to determine energy spectrum and radiative transition probabilities. In Ref. [19], spectra containing transitions in B-like ions were investigated and MCDHF calculations, including some important configurations outside the $n = 2$ complex, were carried out. Vajed-Samii *et al.* in their investigation [11] applied the MCDHF method, allowing nonorthogonality between the radial orbital of the ground $2s^22p$ and excited $2s2p^2$ configurations.

The purpose of the present paper is twofold. First, MCDHF is used to determine $E1$ transition energies, line strengths, transition probabilities, and specific mass shift between the states of the $2s2p^2$ and $2s^22p$ configurations for B-like ions with nuclear charges ranging from $Z = 13$ to 79. These transitions are good candidates not only for testing the quality of the wave functions and further checking many-body atomic theory but also for providing tools for plasma diagnostics. Second, recent observational data has increased the need for accurate atomic data, and given the importance of these transitions in the interpretation of observational results, it therefore seemed desirable to undertake an independent and largely *ab initio* calculation of these lines to see if one set of results can be preferred over the others.

II. METHODS

A. The multiconfiguration Dirac-Hartree-Fock method

The MCDHF method is explained in detail in a recent monograph by Grant [22], and here we give only a brief outline. Starting from the Dirac-Coulomb Hamiltonian

$$H_{\mathrm{DC}} = \sum_{i=1}^{N} \left[c\boldsymbol{\alpha}_i \cdot \boldsymbol{p}_i + (\beta_i - 1)c^2 + V_i^N \right] + \sum_{i<j}^{N} 1/r_{ij}, \quad (1)$$

where V^N is the monopole part of the electron-nucleus Coulomb interaction, the atomic state functions describing different fine-structure levels are obtained as linear combinations of symmetry-adapted configuration state functions (CSFs)

$$\psi(\gamma J M_J) = \sum_j c_j \phi(\gamma_j J M_J). \quad (2)$$

*gjiang@scu.edu.cn

Here J and M_J are the angular quantum numbers, while γ_j denotes other appropriate labeling of the CSFs, for example, parity, orbital occupancy, and coupling scheme. The CSFs $\phi(\gamma_j J M_J)$ are built from products of one-electron Dirac orbitals. In the relativistic self-consistent field procedure, both the radial parts of the Dirac orbitals and the expansion coefficients are optimized to self-consistency. Calculations can be done for single levels, but also for a portion of a spectrum in an extended optimal level (EOL) way where optimization is on a weighted sum of energies.

Here the rest energy has been subtracted out. While calculating the nuclear potential, we have also taken into account the nuclear volume effect by considering the Fermi charge distribution given by

$$\rho_{\rm nuc}(r) = \frac{\rho_0}{1 + e^{(r-c)/a}}, \tag{3}$$

where c is the half-density radius and a is a measure of the skin thickness.

In subsequent relativistic configuration interaction (RCI) calculations, the transverse photon interaction

$$H_{\rm Breit} = -\sum_{i<j}^{N}\left[\frac{\alpha_i \cdot \alpha_j}{2r_{ij}} + \frac{(\alpha_i \cdot r_{ij})(\alpha_j \cdot r_{ij})}{2r_{ij}^3}\right] \tag{4}$$

may be included in the Hamiltonian [23]. The contributions from self-energy and vacuum polarization corrections have also been taken into account in our calculations. The formulas for self-energy and vacuum polarization can be found elsewhere [23].

B. Transition parameters

The transition parameters, such as line strengths and rates, for multipole transitions between two atomic states $\gamma P J M_J$ and $\gamma' P' J' M'_J$ can be expressed in terms of the reduced transition matrix element

$$\langle \psi(\gamma P J) || Q_k^{(\lambda)} || \psi(\gamma' P' J') \rangle, \tag{5}$$

where $Q_k^{(\lambda)}$ is the corresponding transition operator in Coulomb or Babushkin gauges. To compute the transition matrix element between two atomic state functions described by independently optimized orbital sets, biorthogonal transformations of the atomic state functions were performed [24]. In the new representation, the evaluation of the matrix element was done using standard Racah algebra techniques.

III. GENERATION OF CONFIGURATION EXPANSITIONS

From some perspectives, it is desirable to perform separate calculations for each of the studied atomic states. However, this approach is impractical and time-consuming when considering large portions of a spectrum. In this work, the atomic wave functions were generated separately for each term. Within a given term, all fine structure levels were represented by wave functions optimized together in an EOL scheme, where the optimization was on the weighted energy average of the states [25]. For the terms belonging to the $2s^22p$ ground configuration, the configuration expansions were generated by single and double substitutions (SD expansion) from the $\{2s^22p, 2p^3\}$ multireference set to an active set of orbitals. For the terms belonging to the $2s2p^2$ configuration, the configuration lists were generated by SD substitutions from the single reference configuration to an active set of orbitals. Here CSFs of a specified parity and J symmetry are generated by excitations from a number of reference configurations to a set of relativistic orbitals. By applying restrictions on the allowed excitations, different electron correlation effects can be described. In order to monitor the convergence of computed properties, the active sets were systematically enlarged to include orbitals with principal quantum numbers $n = 3...7$ and orbital quantum numbers $l = 0...4$ (i.e., angular symmetries *s, p, d, f, g*); the active sets were done layer by layer of correlation orbitals.

In the present work, valence-valence (VV) and core-valence (CV) electron correlation effects were included to describe inner properties, like fine structure. The theoretical basis of our present computational approach has been discussed in our previous work [26]. In this paper, we give a brief overview of the salient features of the MCDHF model with configuration interaction.

The configuration list was condensed during the optimization stage in order to save computing time. To investigate the effect of higher order correlation effects, RCI calculations including the Breit interaction were performed for expansions where the largest SD expansions (no condensation) were augmented with expansions generated by all possible excitations from the outer shells keeping $1s$ closed. At the final stage, the multireference set for the terms of the $2s^22p$ configuration was enlarged to include $\{2s^22p, 2p^3, 2s2p3d, 2s3d^2\}$. The multireference was chosen based on the criteria that it should contain the configurations that had the largest weights in the preceding self-consistent field calculations. Among the states generated by SD excitations from the multireference set, only those interacting with the multireference states were kept. In the same way, the multireference set for $2s2p^2$ was enlarged to include the configurations $\{2s2p^2, 2p^23d, 2s2p3d, 2p3d^2\}$. The leading QED effects (vacuum polarization and self-energy) were added, as perturbative corrections, to the results of the final multireference RCI calculations.

IV. RESULTS AND DISCUSSION

The success of a calculation relies on a judiciously chosen configuration expansion. To ensure the convergence of a calculated expectation value within a certain correlation model, the configuration expansion must be enlarged in a systematic way. A very efficient way of doing this is to use the active set approach, where *jj*-coupled configuration state functions of a specified parity P and angular momentum J symmetry are generated by excitations from one or more reference configurations to an active set of orbitals. The convergence of the atomic property can then be studied as a function of the size of the active set. To build a reasonable correlation model and control the accuracy, we performed tentative calculations on transition energies and line strengths of the $2s^22p - 2s2p^2\,E1$ transition for B-like isoelectronic sequence. In the calculations, the states of the $2s^22p$ and $2s2p^2$ configurations were optimized layer by layer in an EOL scheme. These calculation were followed by calculations with CSF expansions generated by single (S) and double (D)

TABLE I. Fine-structure energy levels of B-like Fe ($Z = 26$) given relative to the ground level (in cm^{-1}), where $n = 3$ denotes the orbital set with maximal principal quantum number $n = 3$, etc. Results of valence and core-valence correlations include Breit interaction and quantum electrodynamical (QED) effects.

	Valence correlation				Core-valence correlation					Other calculations	
Level	$n=4$	$n=5$	$n=6$	$n=7$	$n=4$	$n=5$	$n=6$	$n=7$	Expt[a]	MCDF[b]	MBPT[c]
$2s^2 2p$											
$^2P_{1/2}$	0	0	0	0	0	0	0	0	0	0	
$^2P_{3/2}$	1 18 160	1 18 162	1 18 164	1 18 165	1 18 272	1 18 343	1 18 351	1 18 359	1 18 266	1 21 890	1 15 443
$2s^2 p^2$											
$^4P_{1/2}$	4 03 750	4 04 574	4 04 753	4 04 811	4 03 311	4 03 928	4 04 284	4 04 298	4 04 550	3 99 255	4 03 328
$^4P_{3/2}$	4 59 161	4 60 086	4 60 282	4 60 345	4 58 544	4 59 599	4 59 996	4 59 991	4 60 190	4 56 484	4 58 172
$^4P_{5/2}$	5 12 417	5 13 241	5 13 426	5 13 487	5 11 830	5 12 606	5 12 984	5 13 115	5 13 260	5 14 131	5 10 567
$^2D_{3/2}$	7 39 220	7 38 003	7 37 946	7 37 926	7 38 519	7 37 027	7 36 933	7 36 798	7 36 310	7 46 814	7 32 518
$^2D_{5/2}$	7 61 798	7 60 706	7 60 663	7 60 659	7 61 154	7 59 831	7 59 771	7 59 548	7 59 210	7 70 515	7 55 453
$^2S_{1/2}$	9 82 648	9 80 811	9 80 576	9 80 525	9 81 924	9 80 037	9 79 351	9 79 223	9 78 350	9 90 703	9 71 284
$^2P_{1/2}$	8 58 152	8 56 486	8 56 294	8 56 254	8 56 951	8 55 089	8 54 155	8 54 132	8 53 650	8 64 137	8 48 212
$^2P_{3/2}$	9 97 034	9 95 582	9 95 460	9 95 437	9 95 301	9 93 589	9 93 088	9 93 093	9 92 320	1 012 078	9 84 644

[a]Taken from Ref. [27].
[b]Ait-Tahar and Grant [28].
[c]Merkelis *et al.* [4].

excitations from the $2s$ and $2p$ shells of the reference configurations $2s^2 2p$ and $2s2p^2$ to the active set in order to consider VV correlations. The active set was systematically increased by adding layers of new orbitals. The largest active set included all relativistic orbitals with $n \leqslant 7$ and $l \leqslant 4$. Due to stability problems in the self-consistent field procedure, the optimization of radial orbitals was done layer by layer (see Table I). Breit interaction as a part of the electron correlations has been taken into account by a RCI calculation in each step.

In relativistic calculations such as those of the MCDHF method, energy levels are classified by J and π states, with the same J^π are further classified by the order of their total energies. For convenience, however, it is natural to use the jj designations for uncoupled transition and energy matrix elements. For example, the second $J^\pi = 2^+$ state for B-like ions is termed $(2s2p^2)^2 P_{1/2}$.

To assist readers in identifying energy levels and locating transitions, we present schematic diagrams of energy levels, with their labels, for B-like ions in Fig. 1. The relative positions of energy levels in these figures resemble those in actual spectra of light ions, although some of these levels are rearranged as Z increases along isoelectronic sequences.

Table I displays the experimental energy levels [27] and the computed transition energies as functions of the increasing active sets and multireference sets for Fe XXIII. The first column in the table represents the largest principal quantum number of the active set involved in each step of the calculation. As can be seen from Table I, the VV correlations have converged when $n = 7$. The valence calculations were followed by RCI calculations. In these calculations, residual CV correlation effects were accounted for by including CSFs obtained by excitations also from the $1s$ shell of the reference configurations to the largest active space ($n = 7, l = 4$). Triple (T) and quadruple (Q) excitations were neglected due to their very small contributions. Comparisons of the VV and CV correlation with other theoretical data [4,28] showed that the largest discrepancies are less than 3%. The effect of the multireference set is comparatively large for the states which were not fully converged with respect to the orbital basis. We noted the large effects of the increased multireference set on the fine-structure splitting of the terms. In Tables II and III, computed energies and fine-structure splitting for Al IX, Mn XXI, Fe XXII, Co XXIII, Ni XXIV, Cu XXV, Zn XXVI, Mo XXXVIII, and Au LXXV are compared with predicted data given by Cheng *et al.* [1], Edlén [29], Myrnas *et al.* [19], and Safronova [3] and recommended by the National Institute of Standard and Technology (NIST) as presented in [27]. Two calculations are presented for each ion. We have used the full set of orbitals available: for one calculation we keep the

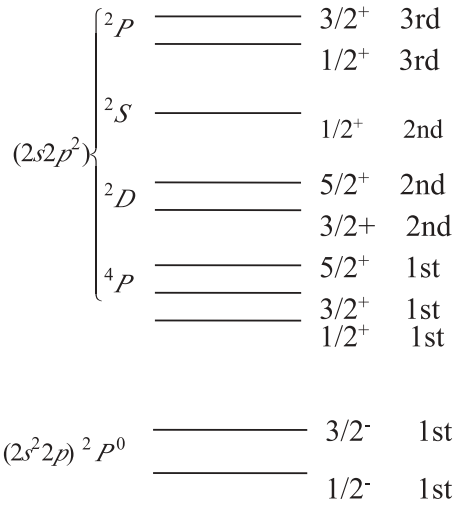

FIG. 1. Conventional spectroscopic notations are shown to the left of the energy levels, with electronic configuration in parentheses, followed by the SL labels ^{2s+1}L. To the right of the energy levels are the MCDF classifications with J^π followed by the nth state with this J^π.

TABLE II. Energy levels (in cm^{-1}) for B-like Al, Mn, Fe, Co, and Ni compared with NIST [27] experiment data.

			Level (cm^{-1})				Splitting (cm^{-1})		
Configuration	Term	J	VV	CV	NIST	Diff.	CV	NIST	Diff%
				$Z = 13$					
$2s^2 2p$	$^2P^o$	0.5	0	0	0	0			
	$^2P^o$	1.5	4 865	4 899	4 890	9	4 899	4 890	0.18
$2s2p^2$	^4P	0.5	1 45 495	1 44 925	1 45 270	−345			
	^4P	1.5	1 47 163	1 46 626	1 46 990	−364	1 701	1 720	−1.10
	^4P	2.5	1 49 656	1 49 114	1 49 460	−346	4 189	4 190	−0.002
	^2D	1.5	2 60 926	2 60 178	2 59 760	418			
	^2D	2.5	2 60 947	2 60 150	2 59 730	420	28	30	−6.67
	^2S	0.5	3 32 951	3 32 652	3 32 710	−58			
	^2P	0.5	3 56 631	3 54 242	3 54 080	162			
	^2P	1.5	3 59 518	3 57 127	3 56 950	177	2 885	2 870	0.52
				$Z = 25$					
$2s^2 2p$	$^2P^o$	0.5	0	0	0	0			
	$^2P^o$	1.5	99 321	99 496	99 360	136	99 496	99 360	0.14
$2s2p^2$	^4P	0.5	3 79 669	3 79 558	3 79 660	−102			
	^4P	1.5	4 24 908	4 24 826	4 24 980	−154	45 268	45 320	0.11
	^4P	2.5	4 70 718	4 70 681	4 70 670	11	91 123	91 010	0.12
	^2D	1.5	6 88 851	6 87 624	6 87 540	85			
	^2D	2.5	7 05 505	7 04 375	7 04 190	185	16 751	16 650	0.61
	^2S	0.5	9 12 799	9 11 123	9 10 880	243			
	^2P	0.5	8 08 534	8 06 382	8 05 930	452			
	^2P	1.5	9 27 733	9 25 075	9 24 710	365	1 18 693	1 18 780	−0.07
				$Z = 26$					
$2s^2 2p$	$^2P^o$	0.5	0	0	0	0			
	$^2P^o$	1.5	1 18 165	1 18 359	1 18 266	93	1 18 359	1 18 266	0.08
$2s2p^2$	^4P	0.5	4 04 811	4 04 298	4 04 550	−252			
	^4P	1.5	4 60 345	4 59 991	4 60 190	−199	55 693	55 640	0.1
	^4P	2.5	5 13 487	5 13 115	5 13 260	−145	1 08 817	10 8710	0.1
	^2D	1.5	7 37 936	7 36 798	7 36 310	488			
	^2D	2.5	7 60 659	7 59 548	7 59 210	338	22 750	22 900	−0.66
	^2S	0.5	9 80 525	9 79 223	9 78 350	873			
	^2P	0.5	8 56 254	8 54 132	8 53 650	482			
	^2P	1.5	9 95 437	9 93 093	9 92 320	773	1 38 961	1 38 670	0.21
				$Z = 27$					
$2s^2 2p$	$^2P^o$	0.5	0	0	0	0			
	$^2P^o$	1.5	1 39 603	1 39 717	1 39 290	427	1 39 717	1 39 290	0.31
$2s2p^2$	^4P	0.5	4 31 887	4 31 206	4 31 560	−354			
	^4P	1.5	4 99 616	4 99 550	4 99 270	280	68 344	67 710	0.94
	^4P	2.5	5 59 615	5 59 587	5 59 760	−173	1 28 381	1 28 200	0.14
	^2D	1.5	7 88 983	7 88 833	7 88 520	313			
	^2D	2.5	8 20 487	8 19 598	8 19 150	448	30 765	30 630	0.44
	^2S	0.5	10 53 397	10 51 465	10 50 860	605			
	^2P	0.5	9 06 160	9 03 476	9 03 260	216			
	^2P	1.5	10 68 176	10 65 050	10 64 960	90	161 574	161 700	0.08
				$Z = 28$					
$2s^2 2p$	$^2P^o$	0.5	0	0	0	0			
	$^2P^o$	1.5	1 63 873	1 64 106	1 63 960	146	1 64 106	1 63 960	0.09
$2s2p^2$	^4P	0.5	4 57 835	4 57 158	4 57 440	−283			
	^4P	1.5	5 39 965	5 39 408	5 39 715	−307	82 250	82 275	−0.03
	^4P	2.5	6 09 271	6 08 745	6 08 975	−230	1 51 587	1 51 535	0.03
	^2D	1.5	8 44 212	8 43 949	8 43 500	449			
	^2D	2.5	8 85 548	8 84 585	8 84 100	485	40 636	40 600	0.09
	^2S	0.5	11 30 908	11 30 042	11 29 710	332			
	^2P	0.5	9 57 539	9 56 102	9 55 790	312			
	^2P	1.5	11 45 468	11 43 364	11 43 250	114	1 87 262	1 87 460	−0.11

TABLE III. Energy levels for B-like Cu, Zn, Mo, and Au from present calculations and compared with experiments and theoretical results.

			Level (cm^{-1})				Splitting (cm^{-1})		
Configuration	Term	J	VV	CV	Ref.[a]	Ref.[b]	CV	Ref.[a]	Ref.[b]
				$Z = 29$					
$2s^2 2p$	$^2P^o$	0.5	0	0					
	$^2P^o$	1.5	1 91 222	1 91 278	1 90 907	1 91 328	1 91 278	1 90 907	1 91 328
$2s2p^2$	^4P	0.5	4 85 635	4 85 590	4 78 278	4 85 800			
	^4P	1.5	5 84 638	5 84 591	5 76 481	5 84 935	99 145	98 203	99 135
	^4P	2.5	6 62 616	6 62 391	6 55 401	6 62 791	1 76 801	1 77 123	1 76 991
	^2D	1.5	9 03 846	9 02 868	9 07 012	9 02 818			
	^2D	2.5	9 56 435	9 55 703	9 57 876	9 55 983	52 836	50 864	53 165
	^2S	0.5	10 13 689	10 11 306	10 18 840	10 11 088			
	^2P	0.5	12 16 572	12 13 769	12 19 979	12 12 218			
	^2P	1.5	12 30 852	12 28 775	12 37 214	12 27 789	15 006	17 235	15 571
				$Z = 30$					
$2s^2 2p$	$^2P^o$	0.5	0	0					
	$^2P^o$	1.5	2 21 914	2 22 191	2 21 481	2 22 021	2 22 191	2 21 481	2 22 021
$2s2p^2$	^4P	0.5	5 14 227	5 13 534	5 06 773	5 14 627			
	^4P	1.5	6 32 931	6 32 370	6 24 489	6 33 460	1 18 836	1 17 716	1 18 833
	^4P	2.5	7 19 843	7 19 295	7 12 570	7 20 201	2 05 761	2 05 797	2 05 574
	^2D	1.5	9 66 127	9 65 134	9 69 050	9 65 237			
	^2D	2.5	10 33 786	10 33 090	10 34 639	10 33 714	67 956	65 589	68 477
	^2S	0.5	10 69 969	10 69 116	10 76 774	10 69 605			
	^2P	0.5	13 06 993	13 03 199	13 10 843	13 02 453			
	^2P	1.5	13 21 903	13 18 858	13 27 820	13 18 873	15 659	16 977	16 420
				$Z = 42$					
$2s^2 2p$	$^2P^o$	0.5	0	0					
	$^2P^o$	1.5	9 63 378	9 64 860	9 59 831	9 64 360[c]	9 64 860	9 59 831	9 63 920
$2s2p^2$	^4P	0.5	8 95 055	8 95 148	8 85 613	8 94 050[c]			
	^4P	1.5	16 04 775	16 06 421	15 92 028		7 11 273	7 06 415	7 10 787
	^4P	2.5	17 91 887	17 92 388	17 83 115	17 90 130[c]	8 97 240	8 97 502	
	^2D	1.5	21 04 598	21 04 466	21 03 022	21 02 900[c]			
	^2D	2.5	27 22 729	27 24 464	27 15 010		6 19 998	6 11 988	6 19 880
	^2S	0.5	21 48 404	21 47 374	21 46 666	21 47 300[c]			
	^2P	0.5	31 63 189	31 63 991	31 58 386	31 64 770[c]			
	^2P	1.5	31 73 198	31 73 563	31 72 346	31 71 300[c]	9572		9602
				$Z = 79$					
$2s^2 2p$	$^2P^o$	0.5	0	0					
	$^2P^o$	1.5	1 59 66 505	1 59 70 713	1 59 68 847	1 59 46 663[d]	1 59 70 713	1 59 68 847	1 59 46 663[d]
$2s2p^2$	^4P	0.5	24 58 545	24 54 264	24 61 301	24 53 135[d]			
	^4P	1.5	1 77 06 572	1 77 07 697	1 76 80 114	1 76 83 142[d]	1 52 53 433	1 52 18 813	1 52 30 007[d]
	^4P	2.5	1 80 45 897	1 80 46 300	1 80 22 562	1 80 20 532[d]	1 55 92 036	1 55 61 261	1 55 67 397[d]
	^2D	1.5	1 87 11 454	1 87 10 791	1 86 91 174	1 86 84 334[d]			
	^2D	2.5	3 38 16 712	3 38 21 897	3 37 66 171	3 37 72 420[d]	1 51 11 106	1 50 74 997	1 50 88 086[d]
	^2S	0.5	1 86 97 609	1 86 96 036	1 86 74 381	1 86 69 953[d]			
	^2P	0.5	3 47 83 499	3 47 88 602	3 47 37 429	3 47 38 035[d]			
	^2P	1.5	3 47 89 703	3 47 93 058	3 47 42 700	3 47 42 092[d]	4456	5271	4057[d]

[a]Cheng *et al.* [1].
[b]Edlén [29].
[c]Myrnas *et al.* [19].
[d]Safronova *et al.* [3].

$1s^2$ shell closed ("valence"), whereas in the other we allow excitations from the $1s$ orbital to others in the set ("core"). For the most part, there is improvement in the agreement with experimental results when core orbital replacements are included. The fine-structure splitting of the states also improves slightly with the inclusion of core correlation. Relative to the ground-state energy, the energies of other states are up to 1000 cm^{-1} in error. This corresponds to less than 1% of the transition energies of both the allowed transitions and the intercombination lines (Table II). From Table III, it is clear that the CV correlation results show excellent agreement with the experiment values of Edlén [29] and Myrnäs *et al.* [19]

TABLE IV. Convergence of the length (S_l) and velocity (S_v) line strength and transition energy between the $2s^2\ 2p^2\ P^o_{1/2}$ and $2s2p^{24}P_{3/2}$ configurations of B-like Al.

	VV			CV		
Active set[a]	S_l	S_v	ΔE (cm^{-1})	S_l	S_v	ΔE (cm^{-1})
2	2.20(−6)	1.82(−6)	141 049	2.20(−6)	2.03(−6)	141 135
3	2.22(−6)	1.91(−6)	146 071	2.28(−6)	2.12(−6)	145 680
4	2.38(−6)	2.15(−6)	146 947	2.35(−6)	2.53(−6)	146 222
5	2.40(−6)	2.09(−6)	147 113	2.38(−6)	2.44(−6)	146 462
6	2.40(−6)	2.08(−6)	147 157	2.39(−6)	2.42(−6)	146 624
7	2.40(−6)	2.07(−6)	147 163	2.39(−6)	2.40(−6)	146 626
Obs.[b]				2.39(−6)		146 990

[a]The orbital active set is specified by the n value.
[b]Taken from [27].

to within a few percentage points (0.1% and 0.03%). Also, our calculations are also generally in good agreement with the MCDF results of Cheng *et al.* [1] and the MBPT data from Safronova [3]. The calculations of Safronova [3] are given in units of the unified electron volts (eV) and can be converted to cm^{-1} for Mo XXXVIII and Au LXXV ions. We have used 1 eV = 8065.5447 cm^{-1}. However, a more detailed comparison of the calculated and experimental energies for these transitions (Table III) indicates that some splitting energies given by our GRASP2 K calculations are in better agreement with experimental energies than the MCDF results of Cheng *et al.* [1]. Specifically, the maximum difference between the results of experiment and our GRASP2 K transition wavelengths is 0.212%, but the maximum difference for the MCDF results of Cheng *et al.* [1] and the experimental results is 1.526%. In the work presented here, we have increased the number of configurations included or the size of the orbital set in a systematic manner until good convergence was obtained. This difference in the two methods should account for a large fraction of the disagreement in the results. From Tables II and III, it is clear that the fine structure for this term is highly irregular along the sequence and is not described very well in the present calculations. The fine-structure splitting is strongly affected by the multireference set and it would be desirable to increase it further.

In Table IV, the line strengths for $2s^2\ 2p\ ^2P^o_{1/2}$–$2s2p^2\ ^4P_{3/2}$ in Al IX are shown as functions of increasing active sets and multireference sets. The results are from the various valence and CV correlation calculations. The convergence of the results is clearly seen as n increases in the two correlation calculations. As can be seen from this table, the agreement of the two gauges is very good and the near-equal values of the length and velocity of the transitions give an additional check on the accuracy of our results. The agreement of the two gauges improves with increasing n. At the same time, we can find that the length value is more stable in that it changes less as the active space extends. For this reason, we use length gauge in our present work. Strengths for all $E1$ transitions in the $2s^22p - 2s2p^2$ transition array are given in Table V.

In Table V, we compare our results for transition energies ΔE, transition rates A_{ki}, the line strengths S_l, and the ratios of velocity to length strengths (S_v/S_l) of B-like ions with nuclear charges ranging from $Z = 13$ to 79. Also, some available theoretical and experimental results are tabulated for comparison. Our comparison is presented in two parts: transition energies and transition probability differences. Our MCDHF values are compared with theoretical values given by Cheng *et al.* [1] and Merkelis *et al.* [4] and with experimental results given by Edlén [29], Myrnas *et al.* [19], and the NIST database [27]. For all Z ions, it is clear that the calculated values including the CV correlation are in general in very good agreement with the MCDF calculation of Cheng *et al.* [1] and the MBPT calculations of Merkelis *et al.* [4], except for some transitions with a maximum difference of approximately 0.28%. A comparison between the present transition energies and the Joint European Torus (JET) tokomak experimental values of Myrnas *et al.* [19] and the NIST database [27] reveals that the greatest difference between the experimental results and our GRASP2 K transition energies for our CV correlation calculations is 0.21%. In the highly ionized atoms, the term structure is best described by *jj* coupling, whereas in the range from the lowest charge states up to the Fe group the *LS* coupling approximation is valid. This is illustrated in Fig. 2, which displays the smoothed data energy levels from Table V. To avoid future level-identification problems, besides transition energies we include in Table V transition rates A_{ki} and line strength S_l. Uncertainties in the accuracy of the A values for these transitions will be determined mainly by the accuracy of the line strength S_l. Our GRASP2 K calculation of the A_{ki} values for the $2s^22p - 2s2p^2$ transition is in excellent agreement with the theoretical and experimental results. In order to check our calculations, the ratios of velocity to length strengths (S_v/S_l) were computed, and we find that most ratios fluctuate around 1. The nearly equal values of the velocity and length rates foremost of the transitions can justify our present calculated results. Since the present transition data are obtained using a single method for all Z and improve in accuracy with increasing Z, we expect our data for high Z to be very reliable.

It is some interest to consider theoretical rates A_J for $2s^2\ 2p\ ^2P_J$–$2s2p^2\ ^2S_{1/2}$ and $2s^2\ 2p\ ^2P_J$–$2s2p^2\ ^2P_{1/2}$ transition for $J = 1/2$ and 3/2. The branching ratio $A_{3/2}/A_{1/2}$ for the former transition is equal to 2 in the *LS*-coupling limit, as is the ratio $A_{1/2}/A_{3/2}$ for the latter transition. Deviation of either ratio from 2 indicates the presence of relativistic (spin-orbit) effects. The spin-orbit interaction for the $2s^2\ 2p\ ^2S_{1/2}$ and $^2P_{1/2}$ levels was discussed by Cheng *et al.* in [1] and

TABLE V. Nonrelativistic transition energies (ΔE in cm^{-1}), transition rates (length formalism, in s^{-1}), the line strengths (in a.u.), and the ratios of velocity to length strengths (S_v/S_l) of B-like ions. Numbers in parentheses are powers of 10.

	Previous		Present (CV)				Previous		Present (CV)			
Z	ΔE	A_{ki}	ΔE	A_{ki}	S_l	S_v/S_l	ΔE	A_{ki}	ΔE	A_{ki}	S_l	S_v/S_l
	$2s^2\ 2p\ ^2P^o_{1/2} - 2s2p^2\ ^4P_{1/2}$						$2s^2\ 2p\ ^2P^o_{1/2} - 2s2p^2\ ^2S_{1/2}$					
13	1.453(5)[a]	1.52(5)[a]	1.449(5)	1.50(5)	4.87(−5)	1.006	3.327(5)[a]	3.98(9)[a]	3.327(5)	4.07(9)	1.08(−1)	0.991
25	3.797(5)[a]	6.1(7)[a]	3.796(5)	5.76(7)	1.04(−3)	0.990	8.059(5)[a]	3.63(10)[b]	8.064(5)	3.46(10)	6.50(−2)	0.998
26	4.046(5)[a]	8.7(7)[a]	4.043(5)	8.54(7)	1.23(−3)	1.032	8.537(5)[a]	3.9(10)[a]	8.541(5)	3.80(10)	6.02(−2)	0.997
27	4.316(5)[a]	1.2(8)[a]	4.312(5)	1.16(8)	1.44(−3)	0.993	9.033(5)[a]	4.3(10)[a]	9.035(5)	4.17(10)	5.56(−2)	0.998
28	4.574(5)[a]	1.7(8)[a]	4.572(5)	1.61(8)	1.66(−3)	1.006	9.558(5)[a]	4.7(10)[a]	9.561(5)	4.67(10)	4.98(−2)	0.998
29	4.858(5)[c]	2.21(8)[b]	4.859(5)	2.19(8)	1.89(−3)	1.011	1.011(6)[c]	5.23(10)[b]	1.011(6)	5.01(10)	4.77(−2)	0.998
30	5.146(5)[c]	2.96(8)[b]	5.135(5)	2.94(8)	2.14(−3)	1.009	1.070(6)[c]	5.72(10)[b]	1.069(6)	5.48(10)	4.42(−2)	1.045
42	8.941(5)[d]	3.21(9)[b]	8.951(5)	3.21(9)	4.42(−3)	1.009	2.147(6)[d]	1.92(11)[b]	2.147(6)	1.89(11)	1.88(−2)	1.005
79		3.09(10)[b]	2.454(6)	3.03(10)	2.03(−3)	1.025		2.44(13)[b]	1.870(7)	2.44(13)	3.68(−3)	1.005
	$2s^2\ 2p\ ^2P^o_{1/2} - 2s2p^2\ ^2P_{1/2}$						$2s^2\ 2p\ ^2P^o_{1/2} - 2s2p^2\ ^4P_{3/2}$					
13	3.541(5)[a]	8.80(9)[a]	3.542(5)	8.84(9)	1.95(−1)	0.990	1.470(5)[a]	3.84(3)[a]	1.466(5)	3.82(3)	2.40(−6)	1.000
25	9.109(5)[a]	3.15(9)[d]	9.111(5)	2.74(9)	3.05(−3)	1.003	4.250(5)[a]	1.35(6)[b]	4.248(5)	1.38(6)	3.56(−5)	1.003
26	9.784(5)[a]	2.7(9)[a]	9.792(5)	2.54(9)	2.44(−3)	1.004	4.602(5)[a]	1.95(6)[b]	4.600(5)	2.00(6)	4.05(−5)	1.005
27	1.051(5)[a]	2.4(9)[a]	1.051(6)	2.34(9)	1.92(−3)	1.005	4.993(5)[a]	2.79(6)[b]	4.996(5)	2.86(6)	4.57(−5)	1.004
28	1.130(6)[a]	2.0(9)[a]	1.130(6)	1.87(9)	1.39(−3)	0.978	5.397(5)[a]	3.96(6)[b]	5.394(5)	4.05(6)	5.10(−5)	1.004
29	1.212(6)[c]	1.83(9)[b]	1.214(6)	1.43(9)	7.86(−4)	1.003	5.849(5)[c]	5.56(6)[b]	5.846(5)	5.69(6)	5.63(−5)	1.011
30	1.302(6)[c]	1.63(9)[b]	1.306(6)	1.29(9)	5.71(−4)	1.003	6.335(5)[c]	7.74(6)[b]	6.324(5)	7.91(6)	6.18(−5)	1.005
42	3.165(6)[d]	5.42(8)[b]	3.165(6)	5.24(8)	1.61(−5)	1.079	3.165(6)[d]	2.27(8)[b]	2.906(6)	2.34(8)	1.11(−4)	1.009
79		3.46(7)[b]	3.479(7)	3.41(7)	2.00(−9)	1.020		2.05(11)[b]	1.771(7)	2.07(11)	7.36(−5)	1.004
	$2s^2\ 2p\ ^2P^o_{1/2} - 2s2p^2\ ^2D_{3/2}$						$2s^2\ 2p\ ^2P^o_{1/2} - 2s2p^2\ ^2P_{3/2}$					
13	2.598(5)[a]	1.64(9)[a]	2.602(5)	1.67(9)	1.87(−1)	0.995	3.569(5)[a]	2.49(9)[a]	3.571(5)	2.53(9)	1.09(−1)	0.991
25	6.875(5)[a]	9.6(9)[a]	6.876(5)	9.23(9)	5.60(−2)	0.996	9.247(5)[a]	6.0(9)[a]	9.251(5)	5.85(9)	1.46(−2)	0.993
26	7.363(5)[a]	1.1(10)[a]	7.368(5)	1.07(10)	5.28(−2)	0.998	9.923(5)[a]	6.20(9)[a]	9.931(5)	6.11(9)	1.23(−2)	0.992
27	7.885(5)[a]	1.3(10)[a]	7.888(5)	1.24(10)	4.99(−2)	0.998	1.065(6)[a]	6.5(9)[a]	1.065(6)	6.36(9)	1.04(−2)	0.990
28	8.435(5)[a]	1.5(10)[a]	8.439(5)	1.44(10)	4.73(−2)	0.998	1.143(6)[a]	6.7(9)[a]	1.143(6)	6.59(9)	8.68(−3)	0.995
29	9.028(5)[c]	1.76(10)[b]	9.029(5)	1.67(10)	4.49(−2)	1.000	1.228(6)[c]	7.02(9)[b]	1.229(6)	6.82(9)	7.26(−3)	0.996
30	9.652(5)[c]	2.04(10)[b]	9.651(5)	1.95(10)	4.27(−2)	1.000	1.319(6)[c]	7.22(9)[b]	1.319(6)	7.05(9)	6.05(−3)	0.995
42	2.103(6)[d]	1.19(11)[b]	2.104(6)	1.16(11)	2.46(−2)	1.004	3.173(6)[d]	1.03(10)[b]	3.174(6)	1.03(10)	6.35(−4)	0.997
79		2.28(13)[b]	1.871(7)	2.26(13)	6.81(−3)	1.003		6.50(10)[b]	3.479(7)	6.69(10)	3.41(−6)	0.994
	$2s^2\ 2p\ ^2P^o_{3/2} - 2s2p^2\ ^4P_{1/2}$						$2s^2\ 2p\ ^2P^o_{3/2} - 2s2p^2\ ^2S_{1/2}$					
13	1.404(5)[a]	1.25(5)[a]	1.400(5)	1.23(5)	4.42(−5)	1.002	3.278(5)[a]	4.19(9)[a]	3.286(5)	4.15(9)	1.13(−1)	0.991
25	2.803(5)[a]	1.3(7)[a]	2.795(5)	1.14(7)	5.16(−4)	1.002	7.063(5)[c]		7.075(5)	2.23(7)	6.21(−5)	0.997
26	2.863(5)[a]	1.4(7)[a]	2.858(5)	1.33(7)	5.63(−4)	1.009	7.354(5)[a]	9.42(7)[e]	7.363(5)	9.18(7)	2.27(−4)	0.996
27	2.923(5)[a]	1.7(7)[a]	2.914(5)	1.67(7)	6.56(−4)	1.003	7.640(5)[a]		7.647(5)	1.98(8)	4.36(−4)	0.993
28	2.935(5)[a]	1.9(7)[a]	2.930(5)	1.84(7)	7.43(−4)	1.004	7.918(5)[a]	1.8(8)[a]	7.926(5)	1.72(8)	3.58(−4)	0.989
29	2.945(5)[c]	1.81(7)[b]	2.934(5)	1.72(7)	6.73(−4)	1.004	8.197(5)[c]		8.204(5)	4.91(8)	8.77(−4)	0.998
30	2.826(5)[c]	1.83(7)[b]	2.923(5)	1.74(7)	6.96(−4)	1.020	8.475(5)[c]		8.479(5)	6.71(8)	1.09(−3)	0.982
42		1.15(5)[b]	6.951(4)	1.09(5)	5.05(−4)	1.008		3.91(9)[b]	1.184(6)	3.97(9)	2.37(−3)	1.013
79		8.16(10)[b]	1.352(7)	8.24(10)	6.59(−5)	0.997		2.18(10)[b]	2.725(6)	2.20(10)	1.07(−3)	1.007
	$2s^2\ 2p\ ^2P^o_{3/2} - 2s2p^2\ ^2P_{3/2}$						$2s^2\ 2p\ ^2P^o_{3/2} - 2s2p^2\ ^4P_{3/2}$					
13	3.521(5)[a]	1.27(10)[a]	3.527(5)	1.29(10)	5.82(−1)	0.990	1.421(5)[a]	3.09(4)[a]	1.417(5)	3.33(4)	2.31(−5)	1.009
25	8.254(5)[a]	4.1(10)[a]	8.261(5)	4.00(10)	1.40(−1)	1.000		5.95(6)[b]	3.248(5)	6.37(6)	3.67(−4)	1.003
26	8.741(5)[a]	4.5(10)[a]	8.749(5)	4.38(10)	1.29(−1)	1.000	3.419(5)[a]	8.6(6)[a]	3.414(5)	8.38(6)	4.16(−4)	1.005
27	9.257(5)[a]	4.9(10)[a]	9.262(5)	4.81(10)	1.20(−1)	0.992	3.600(5)[a]	1.0(7)[a]	3.582(5)	1.09(7)	4.66(−4)	1.004
28	9.793(5)[a]	5.4(10)[a]	9.802(5)	5.28(10)	1.11(−1)	0.991	3.758(5)[a]	1.3(7)[a]	3.753(5)	1.38(7)	5.17(−4)	1.002
29	1.036(6)[c]	6.06(10)[b]	1.037(6)	5.81(10)	1.03(−1)	1.000	3.936(5)[c]	1.66(7)[b]	3.926(5)	1.74(7)	5.68(−4)	1.003
30	1.097(6)[c]	6.66(10)[b]	1.098(6)	6.41(10)	9.56(−2)	1.001	4.114(5)[c]	2.06(7)[b]	4.112(5)	2.16(7)	6.19(−4)	1.006
42	2.207(6)[d]	2.50(11)[b]	2.209(6)	2.46(11)	4.50(−2)	1.000		1.32(8)[b]	6.416(5)	1.35(8)	1.01(−3)	1.010
79		3.57(13)[b]	1.882(7)	3.56(13)	1.05(−2)	1.010		1.40(9)[b]	1.737(6)	1.43(9)	5.34(−4)	1.004

TABLE V. *(Continued.)*

	Previous		Present (CV)				Previous		Present (CV)			
Z	ΔE	A_{ki}	ΔE	A_{ki}	S_l	S_v/S_l	ΔE	A_{ki}	ΔE	A_{ki}	S_l	S_v/S_l
	$2s^2\,2p\,^2P^o_{3/2} - 2s2p^2\,^2D_{5/2}$						$2s^2\,2p\,^2P^o_{3/2} - 2s2p^2\,^2P_{5/2}$					
13	2.548(5)[a]	1.79(9)[a]	2.553(5)	1.81(9)	3.22(−1)	1.000	1.446(5)[a]	1.18(5)[a]	1.442(5)	1.23(5)	1.22(−4)	1.016
25	6.048(5)[a]	5.7(9)[a]	6.052(5)	5.44(9)	7.27(−2)	1.003	3.713(5)[a]	4.8(7)[a]	3.707(5)	5.02(7)	2.92(−3)	1.034
26	6.409(5)[a]	6.2(9)[a]	6.408(5)	5.99(9)	6.61(−2)	1.005	3.950(5)[a]	7.0(7)[a]	3.946(5)	7.03(7)	3.48(−3)	0.986
27	6.799(5)[a]	6.7(9)[a]	6.798(5)	6.38(9)	6.01(−2)	1.003	4.205(5)[a]	1.0(8)[a]	4.192(5)	1.02(8)	4.11(−3)	1.005
28	7.201(5)[a]	7.2(9)[a]	7.207(5)	6.90(9)	5.46(−2)	1.004	4.450(5)[a]	1.4(8)[a]	4.446(5)	1.42(8)	4.77(−3)	1.002
29	7.647(5)[c]	7.91(9)[b]	7.642(5)	7.48(9)	4.97(−2)	1.008	4.715(5)[c]	1.83(8)[b]	4.716(5)	1.93(8)	5.47(−3)	1.004
30	8.117(5)[c]	8.56(9)[b]	8.112(5)	8.13(9)	4.51(−2)	1.009	4.982(5)[c]	2.46(8)[b]	4.981(5)	2.56(8)	6.18(−3)	1.003
42		2.88(10)[b]	1.761(6)	2.81(10)	1.53(−2)	1.013	8.258(5)[d]	1.92(9)[b]	8.275(5)	1.92(9)	9.97(−3)	1.013
79		5.26(10)[b]	1.785(7)	5.21(12)	2.71(−3)	1.015		1.01(10)[b]	2.076(6)	1.02(10)	3.36(−3)	1.012

[a]Taken from [27].
[b]Cheng *et al.* [1].
[c]Edlén [29].
[d]Myrnas *et al.* [19].
[e]Merkelis *et al.* [4].

by the NIST database [27]. The model space for even-parity states with $J = 1/2$ includes three states: $2p_{1/2}2p_{1/2}\,[0]\,2s_{1/2}$, $2p_{1/2}2p_{3/2}\,[1]\,2s_{1/2}$, and $2p_{3/2}2p_{3/2}\,[0]\,2s_{1/2}$. The strong mixing of $2p_{1/2}2p_{1/2}\,[0]\,2s_{1/2}$ and $2p_{1/2}2p_{3/2}\,[1]\,2s_{1/2}$ states was discussed in Refs. [3] and [11]. Figure 3 shows the rate ratio $A(3/2-1/2)/A(1/2-1/2)$ in the $^2P^o - {}^2S$ multiplet and

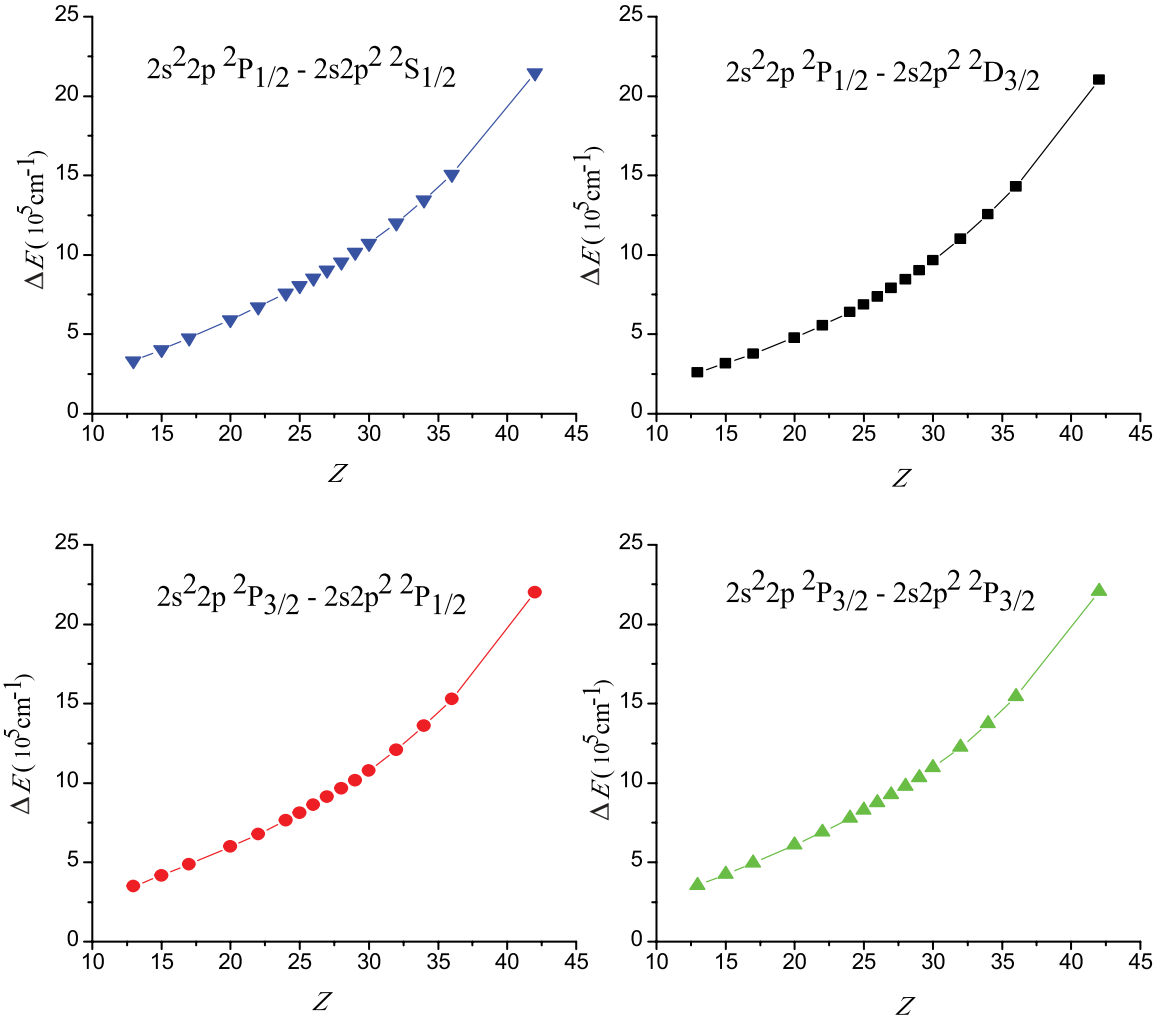

FIG. 2. (Color online) Isoelectronic comparison of the smoothed values of the $2s^22p - 2s2p^2$ $E1$ transition.

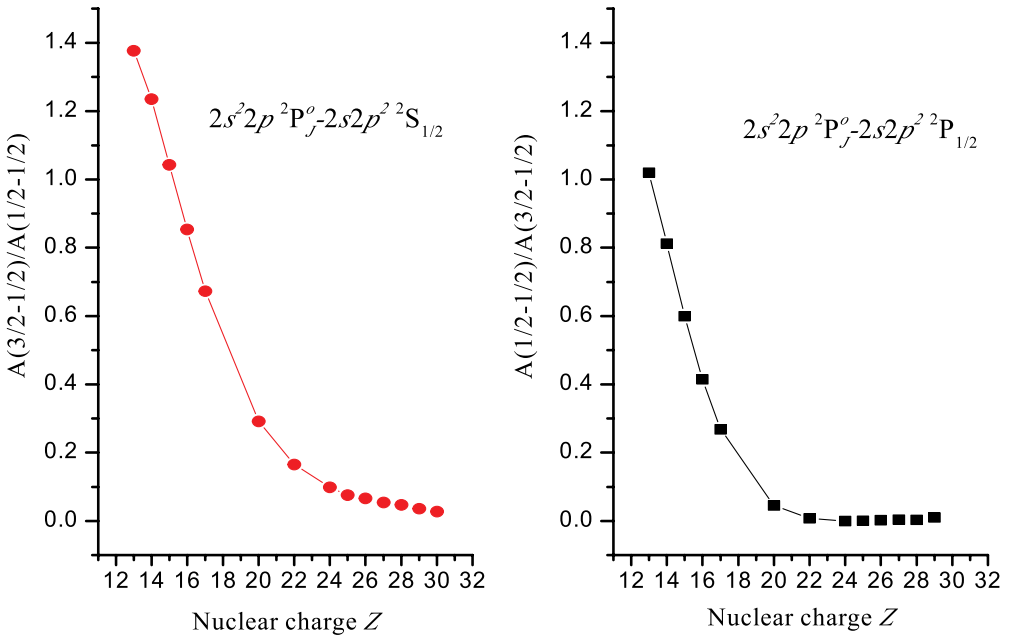

FIG. 3. (Color online) Branching ratios: left panel, $A_{3/2}/A_{1/2}$ for transitions $^2P^o_J - ^2S_{1/2}$; right panel, $A_{1/2}/A_{3/2}$ for transitions $^2P^o_J - ^2P_J$.

$A(1/2-1/2)/A(3/2-1/2)$ in the $^2P^o - ^2P$ multiplet. Lines of the $^2P^o - ^2S$ and the $^2P^o - ^2P$ transition multiplet are blended in several elements, as has been mentioned previously. Data after correction for spectrally unresolved blends are taken into account on the basis of the calculated relative rates in the blending foreign multiplets. This approximation relies on statistical-level populations and the assumption that configuration interaction is less important in the blending multiplets than it is in the B-like spectrum. The uncertainty of the relative detection efficiency (about 10%) is not included in the error bars. The branching ratio of the $^2P^o_J - ^2S_{1/2}$ and $^2P^o_J - ^2P_{1/2}$ transition decrease with increasing Z and become nearly a constant for $Z > 24$. Although the overall behavior in shifting these lines is similar for both the $^2P^o_J - ^2P_{1/2}$ resonance and $^2P^o_J - ^2S_{1/2}$ intercombination transition, the latter is typically more pronounced than the $^2P^o_J - ^2P_{1/2}$ resonance line for the range of $Z = 13$–24. It should be noted that the data given in our paper provided the first systematic study of line intensity ratios and served as a probe of intermediate coupling in the B-like system.

V. CONCLUSION

We have undertaken an extensive and systematic study of the $2s^22p - 2s2p^2$ transitions in B-like ions with $13 \leqslant Z \leqslant 79$ calculated using the GRASP2 K package based on the MCDHF method. Core-valence correlation effects were handled in a systematic way. The Breit interaction and QED effects further corrected the atomic state function and corresponding energy.

The present calculated fine-structure energy levels, term splitting, transition energies, transition rates, line strengths, and thereby the branching ratios were compared with other theoretical and experimental values. Good agreement was found for high- and medium-charged ions, whereas the discrepancies become more obvious with increasing atomic number Z. Taken along with the independent MCDF study by Cheng *et al.* [1], our results show a clear preference for the experimental results of the NIST database [27] over the earlier values of Safronova [3]. These calculations provide a theoretical benchmark for comparison with experiment and theory. For all Z ions (see Tables I–IV), it is clear that the MCDHF method, including the core-valence correlation, is an accurate approach for the whole sequence. It is in general clear that the relativistic and configuration interaction effects play important roles in the correct assignment of different transitions and also in the accurate evaluation of atomic transition data of highly ionized atoms. We hope that these results will be useful in analyzing older experiments and planning new ones.

ACKNOWLEDGMENTS

The authors are grateful to P. Jönsson for providing the GRASP2 K and ATSP2 K packages and giving us many useful instructions. This work was supported by the Nation 863 High-Tech Project Fund.

[1] K. T. Cheng, Y. K. Kim, and J. P. Desclaux, At. Data Nucl. Data Tables **24**, 111 (1979).
[2] U. I. Safronova, W. R. Johnson, and A. E. Livingston, Phys. Rev. A **60**, 996 (1999).
[3] M. S. Safronova, W. R. Johnson, and U. I. Safronova, Phys. Rev. A **54**, 2850 (1996).
[4] G Merkelis, M. J. Vilkas, G. Gaigalas, and R. Kisielius, Phys. Scr. **51**, 233 (1995).

[5] P Jönsson, C. Froese Fischer, and M. S. Godefroid, J. Phys. B **29**, 2393 (1996).
[6] G. Tachiev and C. Froese Fische, J. Phys. B: At. Mol. Opt. Phys. **33**, 2419 (2000).
[7] M. R. Godefroid, C. Froese Fischer, and P. Jönsson, Phys. Scr. T **65**, 70 (1996).
[8] K. D. Lawson, N. J. Peacock, and M. F. Stamp, J. Phys. B **14**, 1929 (1981).
[9] C. Froese Fischer, Phys. Scr. **49**, 323 (1994).
[10] T. Brage, C. Froese Fischer, and P. G. Judge, Astrophys. J. **445**, 457 (1995).
[11] M. Vajed-Samii, D. Ton-That, and L. Armstrong Jr., Phys. Rev. A **23**, 3034 (1981).
[12] H. L. Zhang and D. H. Sampson, At. Data Nucl. Data Tables **56**, 41 (1994).
[13] P. Jönsson, J. G. Li, G. Gaigalas, and C. Z. Dong, At. Data Nucl. Data Tables **96**, 271 (2010).
[14] U. I. Safronova, W. R. Johnson, and M. S. Safronova, At. Data Nucl. Data Tables **69**, 183 (1998).
[15] C. Froese Fischer and G. Tachiev, At. Data Nucl. Data Tables **87**, 1 (2004).
[16] H. S. Nataraj, B. K. Sahoo, B. P. Das, R. K. Chaudhuri, and D. Murherjee, J. Phys. B: At. Mol. Opt. Phys. **40**, 3153 (2004).
[17] K. M. Aggarwal, F. P. Keenan, and K. D. Lawson, At. Data Nucl. Data Tables **94**, 323 (2008).
[18] J. H. Dave, U. Feldman, J. F. Seely, A. Wouters, S. Suckewer, E. Hinnov, and J. L. Schwob, J. Opt. Soc. Am. B **4**, 635 (1987).
[19] R. Myrnäs, C. Jupen, G. Miecnik, I. Martinson, and B. Denne-Hinnov, Phys. Scr. **49**, 429 (1994).
[20] P. Beiersdorfer, D. Knapp, R. E. Marrs, R. E. Elliott, and M. H. Chen, Phys. Rev. Lett. **71**, 3939 (1993).
[21] P. Beiersdorfer, A. Osterheld, S. R. Elliott, M. H. Chen, D. Knapp, and K. Reed, Phys. Rev. A **52**, 2693 (1995).
[22] I. P. Grant, *Relativistic Quantum Theory of Atoms and Molecules* (Springer, New York, 2007).
[23] I. P. Grant, B. J. McKenzie, and P. H. Norrington, Comput. Phys. Commun. **21**, 207 (1980).
[24] J. Olsen, M. Godefroid, P. Jönsson, P.-Å. Malmqvist, and C. Froese Fischer, Phys. Rev. E **52**, 4499 (1995).
[25] K. G. Dyall, I. P. Grant, C. T. Johnson, F. A. Parpia, and E. P. Plummer, Comput. Phys. Commun. **55**, 425 (1989).
[26] L. H. Hao, G. Jiang, and H. J. Hou, Phys. Rev. A **81**, 022502 (2010).
[27] The NIST atomic spectra collection, [http://physics.nist.gov/PhysRefData/ASD/levels_form.html].
[28] S. Ait-Tahar, I. P. Grant, and P. H. Norrington, Phys. Rev. A **54**, 3984 (1996).
[29] B. Edlén, Phys. Scr. **28**, 483 (1983).